Supporting Information

In-situ Growth of $MoSe_2$/Mo Counter Electrode for High Efficiency Dye-sensitized Solar Cells

Haijie Chen,‡[a,b] Yian Xie,‡[a,b] Houlei Cui,[a] Wei Zhao,[a] Xiaolong Zhu,[a] Yaoming Wang,[a] Xujie Lü,[c] and Fuqiang Huang[a,b,*]

[a] *CAS Key Laboratory of Materials for Energy Conversion and State Key Laboratory of High Performance Ceramics and Superfine Microstructures, Shanghai Institute of Ceramics, Chinese Academy of Sciences, Shanghai 200050, People's Republic of China*
[b] *State Key Laboratory of Rare Earth Materials Chemistry and Applications, College of Chemistry and Molecular Engineering, Peking University, Beijing 100871, People's Republic of China*
[c] *High Pressure Science and Engineering Center (HiPSEC), University of Nevada, Las Vegas, Nevada 89154, USA*

* Corresponding author. Fax: +86-21-52416360. Email: huangfq@mail.sic.ac.cn.

Experimental details

Preparation of Mo thin films: The Mo thin film was prepared by the same method in our former report.[1] The Mo films were deposited onto the glass substrates by DC planar magnetron sputtering a 3 inch Mo target at 160 W in Ar atmosphere at 1.2 Pa.

Fabrication of $MoSe_2$/Mo counter electrode (CE) and DSSC: The obtained substrates were then selenized in Se atmosphere to synthesize $MoSe_2$/Mo structure at 500 °C for 10 min, 30 min and 60 min, respectively. The FTO substrates were screen printed with 12 μm thick transparent films of 20 nm-sized TiO_2 particles for the

utilization as photoanodes. The TiO_2 films were sintered in dry air at 450 °C for 30 min. Subsequently, the electrodes were immersed in 40 mM of $TiCl_4$ aqueous solution at 70 °C for 30 min. After sintered in dry air at 450 °C for 30 min again, the electrodes were immersed into a 0.3 mM solution of ruthenium dye N719 in anhydrous ethanol overnight to obtain the photoanodes. The electrolyte was consisted of 0.1 M LiI, 0.05 M I_2, 0.3 M 1,2-dimethyl-3-propylimidazolium iodine, and 0.5 M tert-butylpyridine in 3-methoxypropionitrile. Pt sputtered FTO and the obtained $MoSe_2$/Mo structure were used as CEs. The Pt supported CE was prepared by sputtering Pt onto FTO followed by annealing at 450 °C for 30 min. A DSSC was assembled with a photoanode and CE clipping in the electrolyte solution with a sandwich type arrangement. The active area was 0.25 cm^2. The symmetric cell configuration with an effective area of 0.30 cm^2 for EIS spectra assembled with two identical CEs sandwiching the electrolyte.

Instrumentation: The structure characters were confirmed by the X-ray diffraction (Bruker D8 Focus) using Cu K_α radiation (λ = 1.5418 Å) with the 2θ range from 10° to 80°. SEM images and EDS analysis were taken on a JEOL JSM-6400F microscope equipped with an EDS analytical system. Photocurrent density–voltage characteristics were measured using a Keithley Model 2440 source meter under AM 1.5 illumination. Cyclic voltammetry (CV) was carried out in a three-electrode system which contained 0.1 M $LiClO_4$, 10 mM LiI, 1 mM I_2 at a scan rate of 50 mV $s^{-1}$with a CHI660B electrochemical workstation. The Pt/FTO or $MoSe_2$/Mo served as the working electrode, Pt as the CE and Ag/AgCl as the reference electrode. The

electrochemical impedance spectroscopy (EIS) measurements were performed with a computer-controlled potentiostat (Solartron1287, UK) in the dark by applying an AC voltage with 10 mV amplitude in the frequency range from 0.01 Hz to 100 kHz. The spectra were fitted by the Zview software.

Figure Captions

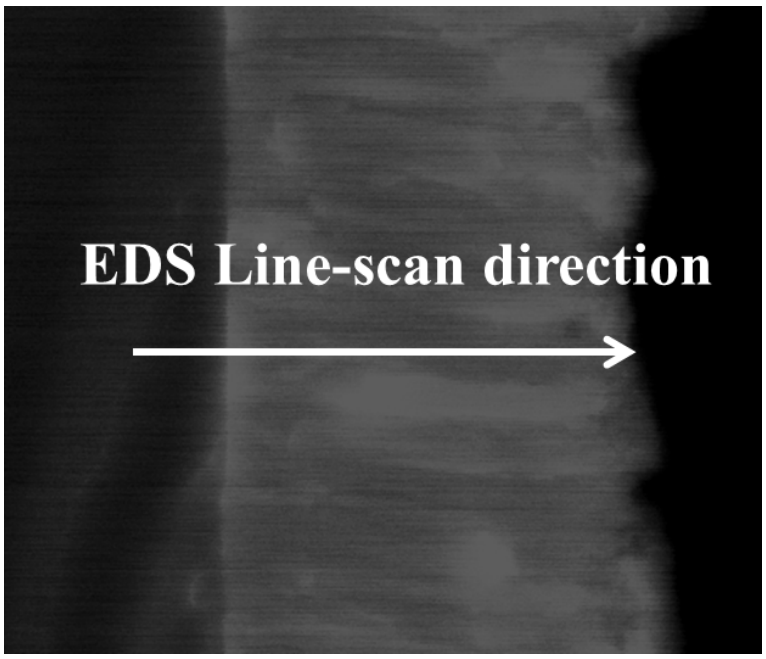

Fig. S1 The cross sectional image for EDS line-scan of the $MoSe_2$/Mo structure.

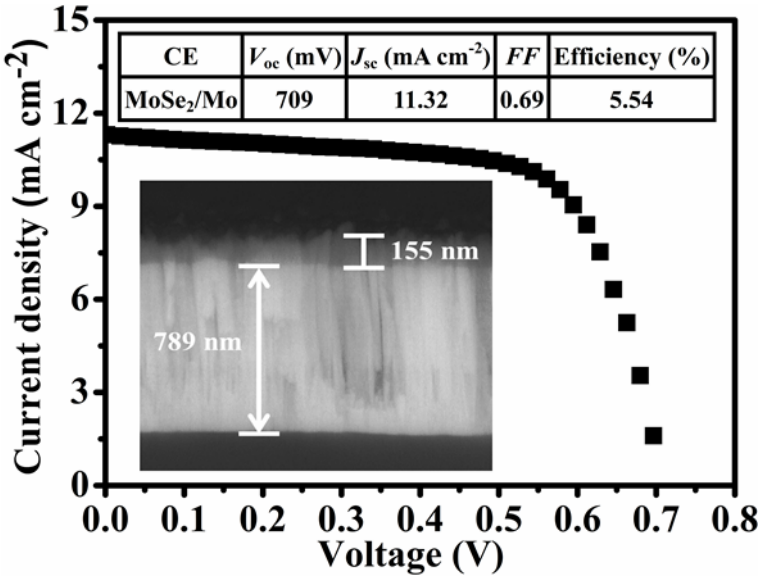

Fig. S2 Photovoltaic performance of DSSC based on $MoSe_2$/Mo CE prepared at 500 °C for 10 min.

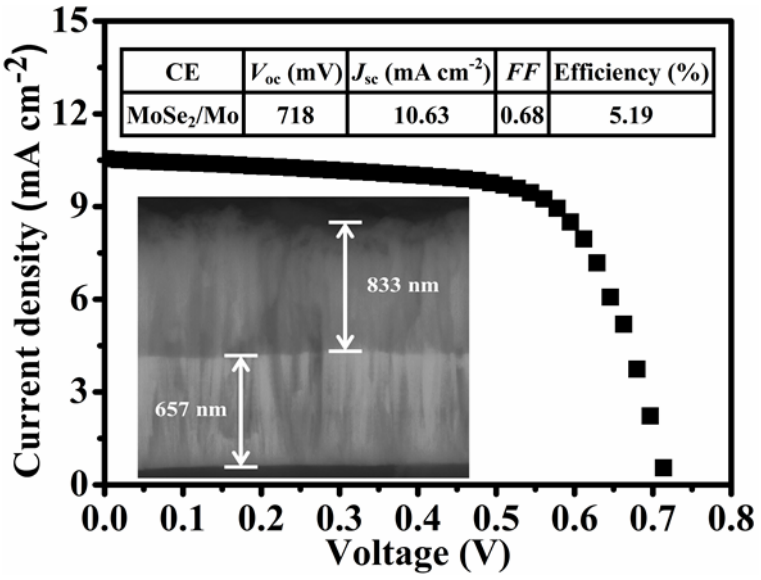

Fig. S3 Photovoltaic performance of DSSC based on $MoSe_2$/Mo CE prepared at 500 °C for 60 min.

The selenization process with different times (10 min, 60 min) at 500 °C and the corresponding DSSCs were also assembled. As shown in Figure S2, the $MoSe_2$ layer with a thickness of 155 nm is presented. The DSSC with this CE generated an efficiency of 5.54 % with short-circuit photocurrent density (J_{sc}) = 11.32 mA cm^{-2}, open circuit voltage (V_{oc}) = 709 mV, and fill factor (*FF*) = 0.69. In Figure S2, the $MoSe_2$ layer is thicker (833 nm), yielding an efficiency of 5.19 % in the corresponding DSSC with J_{sc} = 10.63 mA cm^{-2}, V_{oc} = 718 mV, and *FF* = 0.68. Both of the photovolatic performances of the two DSSCs are worse than that in the manuscript (6.88%, J_{sc} = 13.67 mA cm^{-2}, V_{oc} = 709 mV, and *FF* = 0.71).

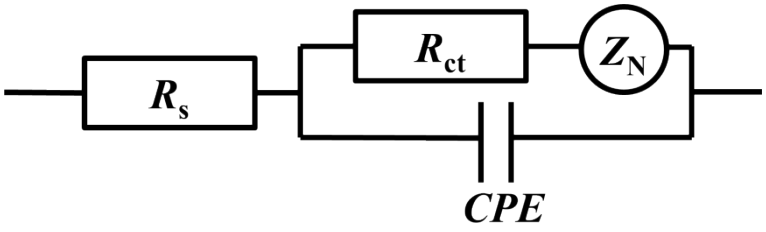

Fig. S4 The corresponding circuit of the Nyquist plots.

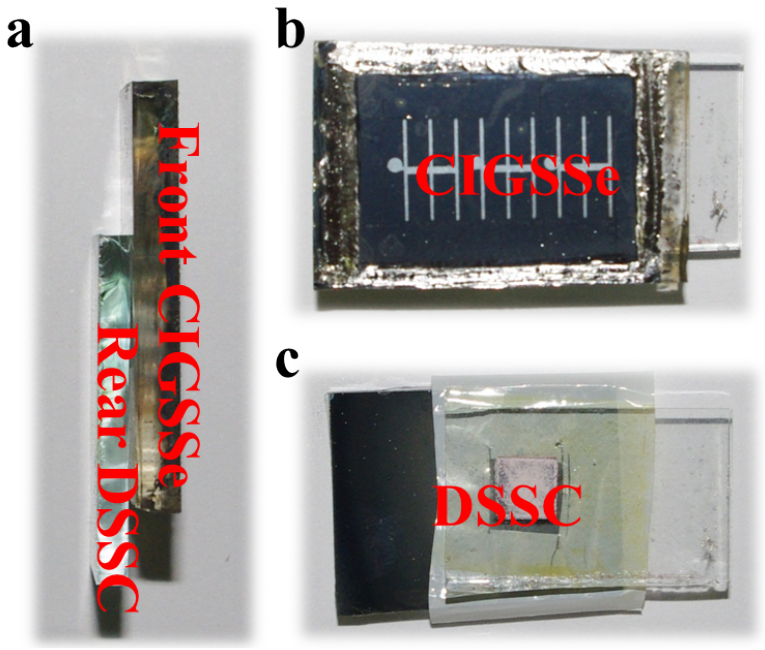

Fig. S5 Photographs of the bifacial solar cell.

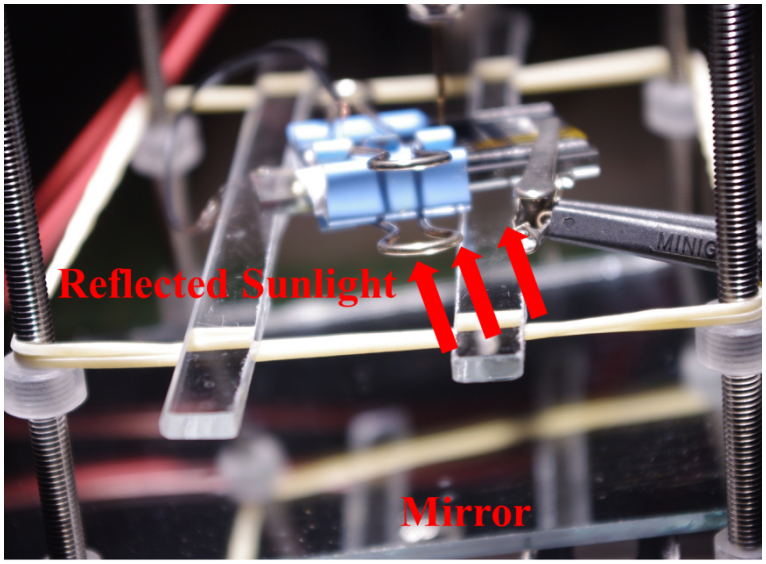

Fig. S6 A photograph of the connected tandem solar cell in series.

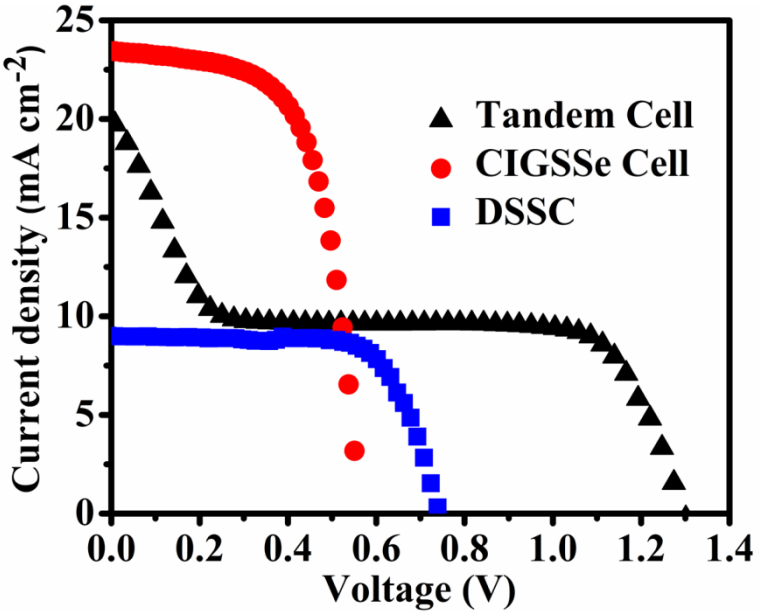

Fig. S7 Photovoltaic performance of the tandem cell.

Table S1. Photovoltaic parameters of the front, the rear and the tandem solar cells.

Cells	J_{sc} **(mA cm^{-2})**	V_{oc} **(mV)**	***FF***	η **(%)**
CIGSSe	23.41	561	0.64	8.39
DSSC	8.95	742	0.72	4.78
Tandem	19.81	1303	0.37	9.83

In order to fabricate a bifacial solar cell, we sputtered Mo onto both sides of the glass substrate, which followed by selenization to form $MoSe_2$/Mo/glass/Mo/$MoSe_2$ structure. The front side was for CIGSSe solar cell and the rear one was for DSSC (Figure S5). We further tried to connect the negative electrode of DSSC (photoanode)

to the positive electrode of CIGSSe cell (the $MoSe_2$/Mo substrate) by a copper wire. Partial of the top cell was covered in order to make the active area accord with that of DSSC (0.25 cm^2). A mirror was located underneath DSSC to reflect sunlight onto the surface of the bottom DSSC (Figure S6). Figure S7 shows the detected photovoltaic performance of the tandem solar cell. Table S1 lists the corresponding photovoltaic parameters. This tandem solar cell generates a high open-circuit voltage (1.30 V), which is the sum of those of the two subcells (0.56 V and 0.74 V).

Reference

R1. X. L. Zhu, Z. Zhou, Y. M. Wang, L. Zhang, A. M. Li and F. Q. Huang, *Sol. Energy Mater. Sol. Cells*, 2012, **101**, 57.